

# Muon imaging and monitoring applied to hydrogeological studies at the Mont Terri Underground Rock Laboratory, Switzerland

M. Tramontini<sup>1,\*</sup>, M. Rosas-Carbalal<sup>2</sup>, C. Nussbaum<sup>3</sup>, F. I. Zyserman<sup>1</sup>, J. Marteau<sup>4</sup>

<sup>1</sup>CONICET - Universidad Nacional de La Plata, Argentina. (UNLP)

<sup>2</sup>Institut de Physique des 2 Infinis de Lyon, Francia. (IP2I)

<sup>3</sup>Swiss Geological Survey at swisstopo.

<sup>4</sup>Institut de Physique du Globe de Paris, Francia. (IPGP)

\*mtramontini@fcaglp.unlp.edu.ar



Facultad de Ciencias  
**Astronómicas**  
y Geofísicas  
UNIVERSIDAD NACIONAL DE LA PLATA



# Outline

- Introduction
- Methodology
- Results
- Conclusions

# Outline

- Introduction
- Methodology
- Results
- Conclusions

# Introduction - About the experiment

- We analyze the data sets of two muography experiments carried out using a portable muon detector at the **Mont Terri Underground Rock Laboratory (URL)**, Switzerland.
  - The objective of these experiments is to evaluate the potential of muography to quantify groundwater variations.
-

# Introduction - About the experiment

- We analyze the data sets of two muography experiments carried out using a portable muon detector at the Mont Terri Underground Rock Laboratory (URL), Switzerland.
  - The objective of these experiments is to evaluate the potential of muography to quantify groundwater variations.
- 

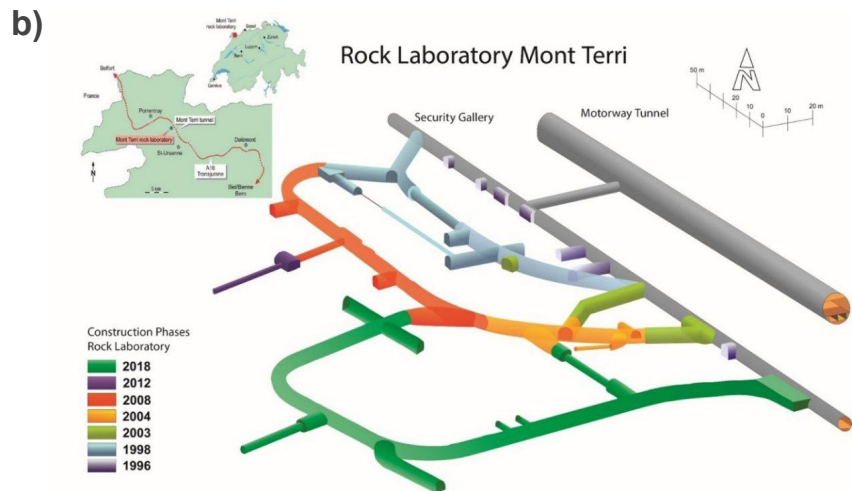
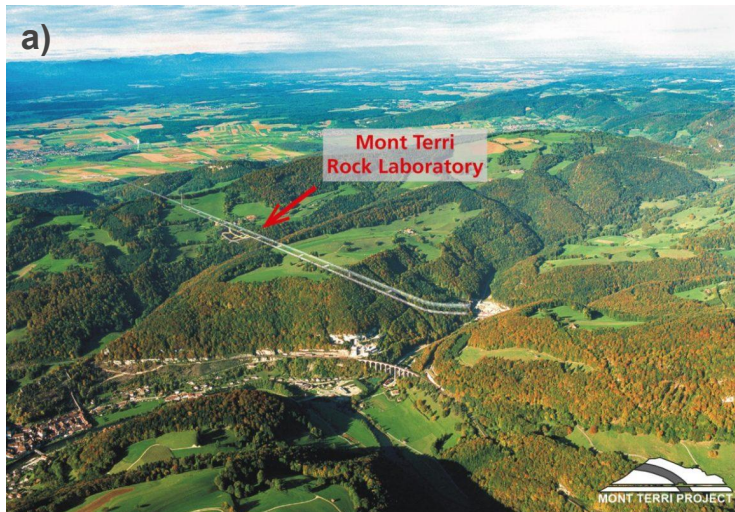
- The portable muon detector was conceived for geoscience applications by the **DIAPHANE** project ([www.diaphane-muons.com](http://www.diaphane-muons.com)).
- It is equipped with 3 plastic scintillator matrices of 80cmx80cm, which are divided into **pixels** that define the **axes of observation of the detector**.

*Portable muon detector deployed in the Mont Terri URL.*



# Introduction - About the Mont Terri URL

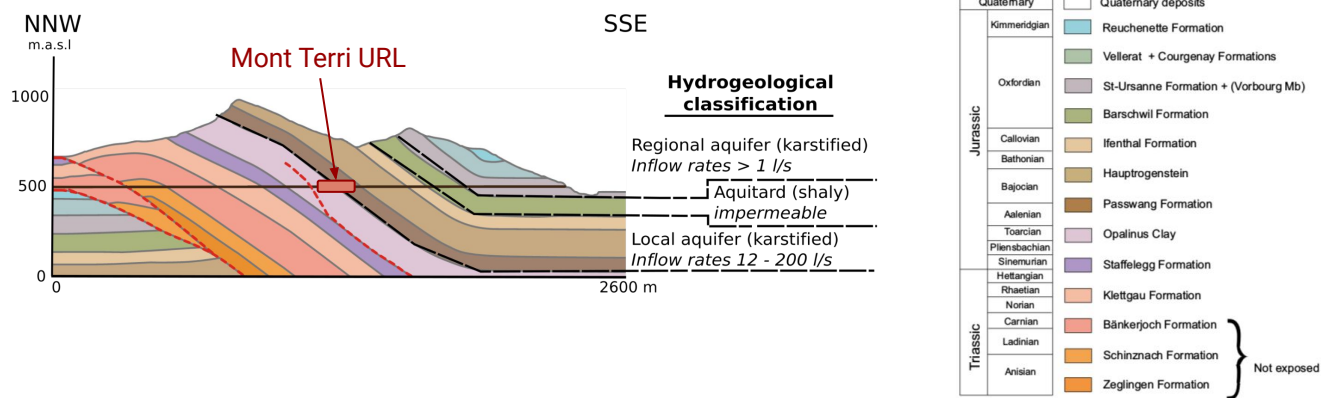
- The **Mont Terri URL** is an international research facility located north of St-Ursanne, Switzerland, at a depth of ~300 m below the Mont Terri mountain.



a) Picture of the site. b) Schematic view of the Mont Terri URL. Images from <https://www.mont-terri.ch/>

# Introduction - About the study region

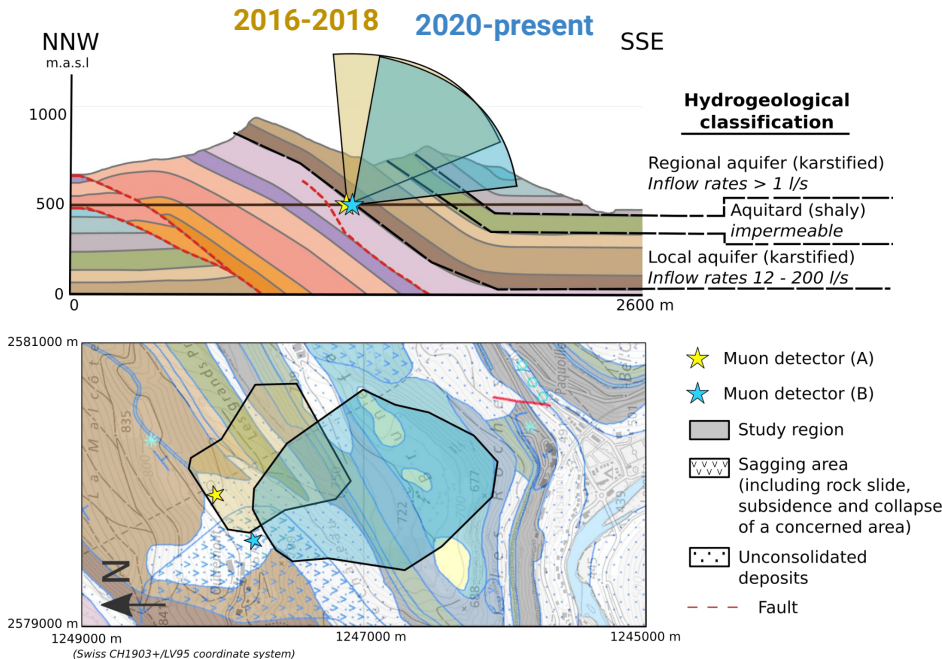
- The **Mont Terri URL** is a key test site for **muography** applied to **hydrogeological studies**: the region hosts **two aquifers**.



*Geological profile modified from Bossart, P. et al. (2018). Hydrogeological classification from Heitzmann, P., editor (2004)*

# Introduction - About the study region

- The Mont Terri URL is a key test site for muography applied to hydrogeological studies: the region hosts two aquifers.



Quaternary	Quaternary deposits
Kimmeridgian	Reuchenette Formation
Oxfordian	Vellerat + Courgenay Formations
Callovian	St-Ursanne Formation + (Vorbourg Mb)
Bathonian	Barschwil Formation
Bajocian	Ifenthal Formation
Aalenian	Hauptrogenstein
Toarcian	Passwang Formation
Pliensbachian	Opalinus Clay
Sinemurian	Staffellegg Formation
Hettangian	Klettgau Formation
Rhaetian	Bänkerjoch Formation
Norian	Schinznach Formation
Carnian	Zeglingen Formation
Ladinian	
Anisian	

Geological profile modified from Bossart, P. et al. (2018). Geological map based on the Geological Atlas of Switzerland 1:25000, available through <https://map.geo.admin.ch>. Hydrogeological classification from Heitzmann, P., editor (2004)

# Outline

- Introduction
- Methodology
- Results
- Conclusions

# Methodology

## Muon imaging

- From the measured muon flux, we calculate the average density along the axes of observation of the muon detector → **muon radiography**.
  - We use an open sky muon flux model derived from air showers simulations using the CORSIKA code (Heck et al. 1998).
  - The muon minimum energy for crossing a given opacity is estimated using attenuation constants given by the Particle Data Group tables.

## Muon monitoring

- We first study the influence of the middle-atmosphere temperature variations in the muon data set in order to remove it from the muon rate variations time series.
- 

- Seasonal variations in the muon rate,  $R$ , caused by the temperature changes in the atmosphere, can be treated in terms of an effective temperature (Barret et al. 1952),  $T_{\text{eff}}$ :

$$\frac{\Delta R}{\langle R \rangle} = \alpha_T \frac{\Delta T_{\text{eff}}}{\langle T_{\text{eff}} \rangle}, \quad \left| \begin{array}{l} \Delta R = R - \langle R \rangle \\ \Delta T_{\text{eff}} = T_{\text{eff}} - \langle T_{\text{eff}} \rangle \end{array} \right.$$

where  $\alpha_T$  is the effective temperature coefficient.

- $T_{\text{eff}}$  is a weighted mean of the atmosphere's temperature profile, and is associated to the altitudes where observed muons are produced (Grashorn et al. 2010). For temperature data, we use the ERA5 data set offered by the ECMWF.

# Methodology

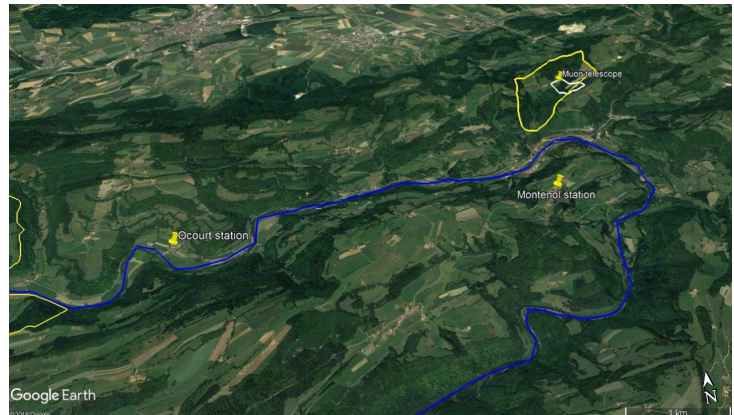
## Muon monitoring (cont.)

- We estimate  $\alpha_T$  following Adamson et al. (2014), and we remove the variations in the muon rate due to the temperature changes in the atmosphere by:

$$\left( \frac{\Delta R}{\langle R \rangle} \right)_{filtered} = \frac{\Delta R}{\langle R \rangle} - \alpha_T \frac{\Delta T_{eff}}{\langle T_{eff} \rangle}$$

- We merge several axis of observation to characterize different regions, and we compare the resulting muon rate variations with rainfall and the Doubs river streamflow.

*Mont Terri's placemarks. The study zone and the associated basin are represented in white and yellow, respectively. The Doubs river is highlighted in blue.*

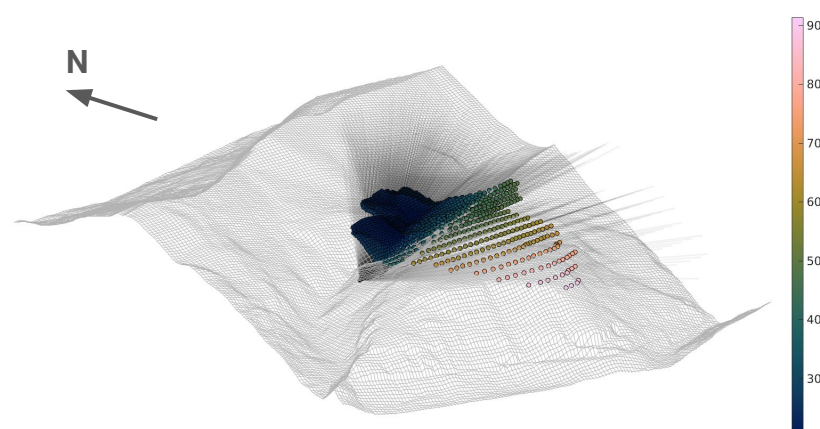
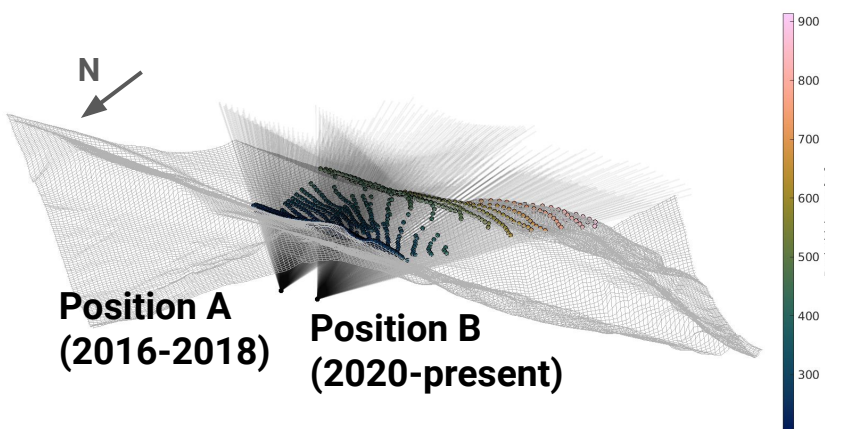


# Outline

- Introduction
- Methodology
- Results
- Conclusions

# Results - Muon imaging

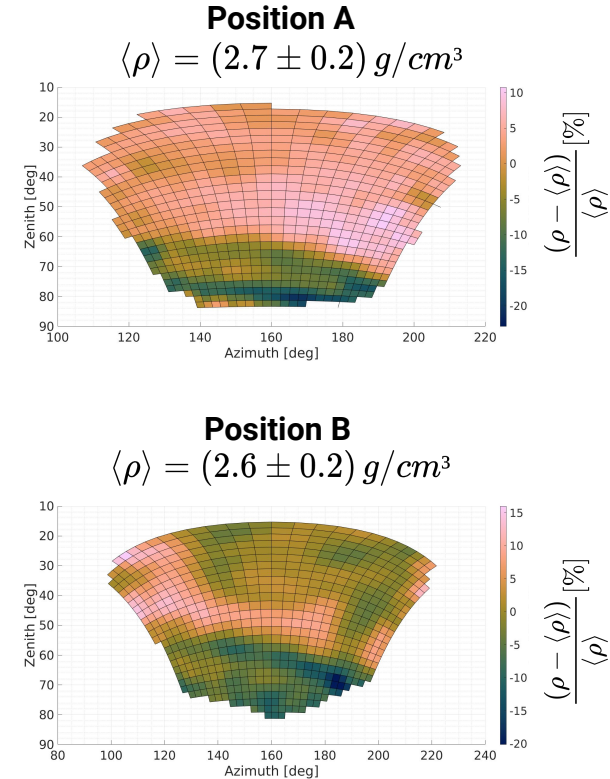
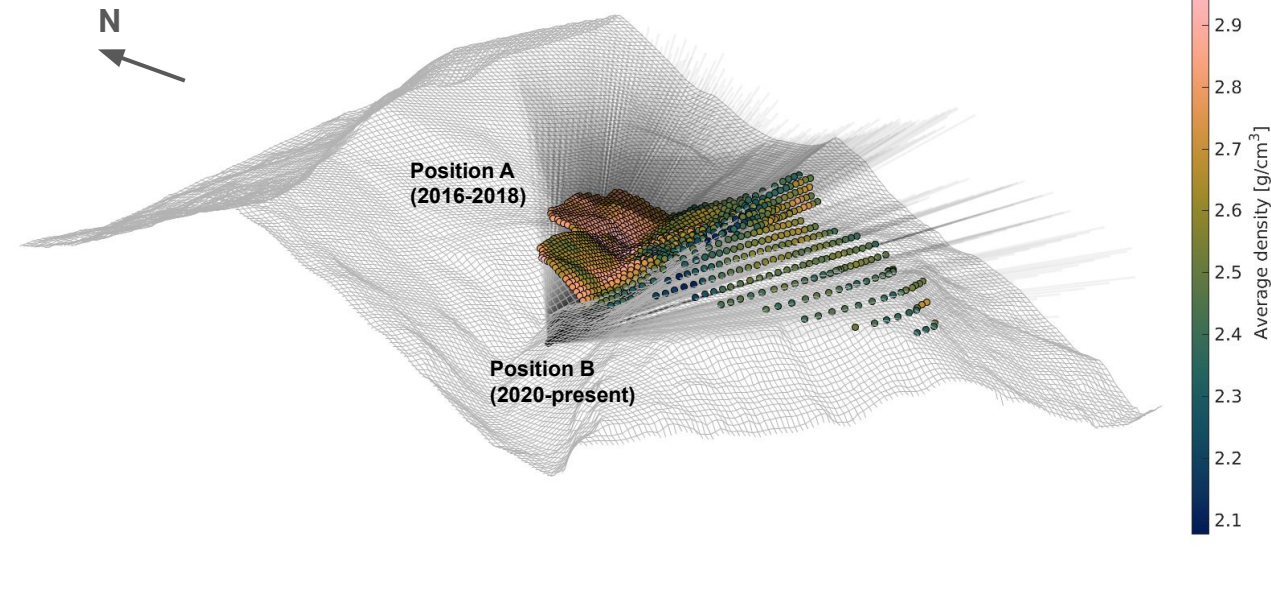
## Rock thickness involved in each experiment



- Position A:  $\langle \text{rock thickness} \rangle = (300 \pm 100) \text{ m}$
- Position B:  $\langle \text{rock thickness} \rangle = (440 \pm 250) \text{ m}$

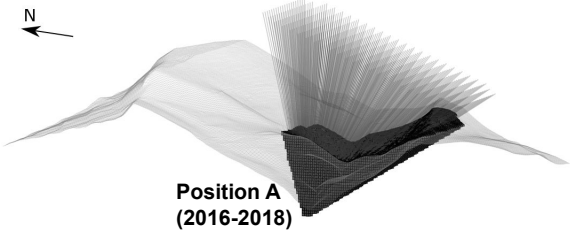
# Results - Muon imaging

- In both experiments, we identified two distinct regions at each side of the valley, a higher density region to the north and a lower one to the south.

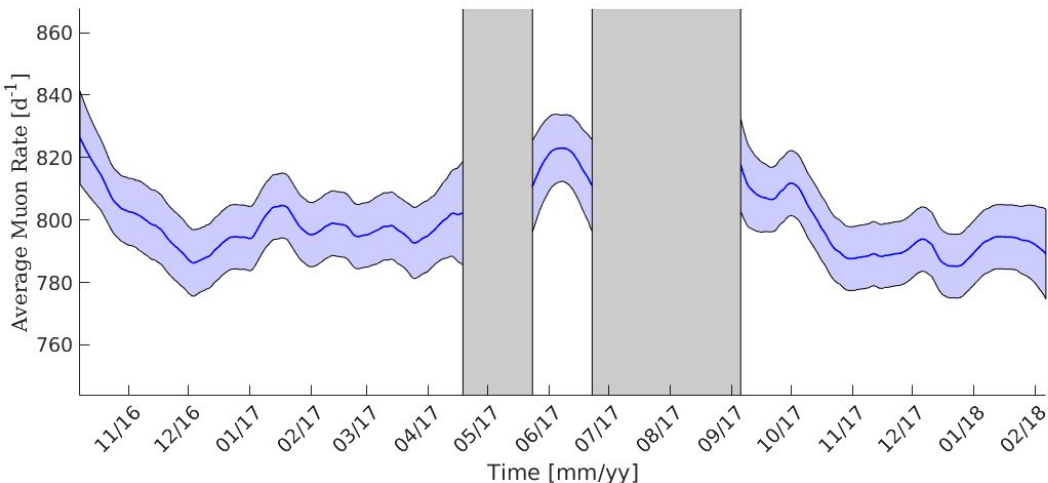


# Results - Muon monitoring

- The average daily rate of muons at  $(675 \pm 160)$  mwe is  $(800 \pm 10) \text{ d}^{-1}$ , based on 382 days of data.



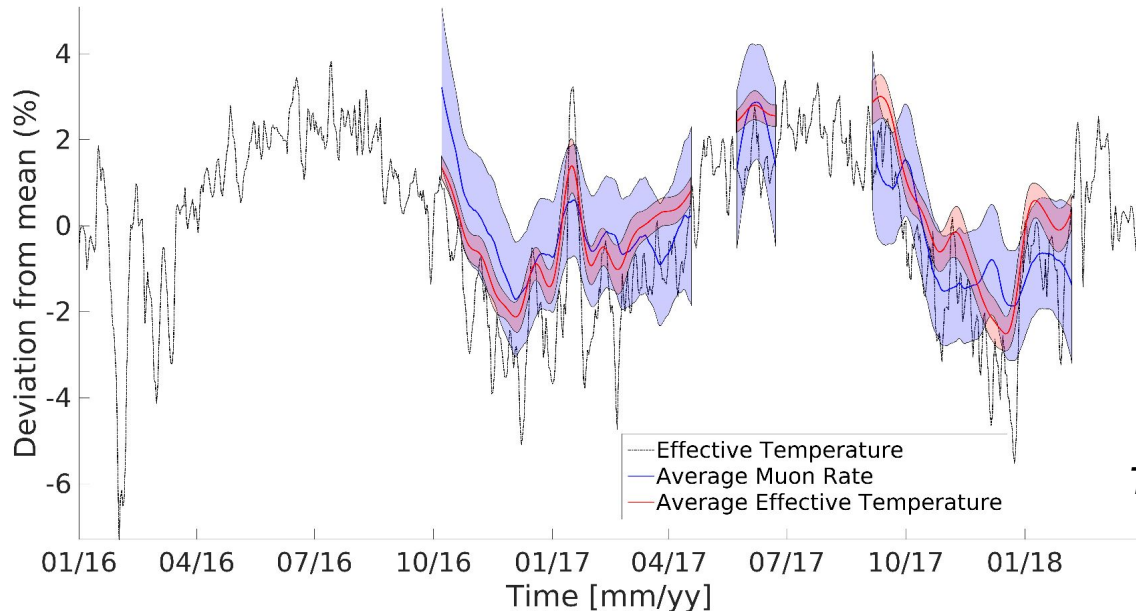
**Study region**  
Volume:  $\sim 11.0 \times 10^6 \text{ m}^3$   
 $\langle \rho \rangle = (675 \pm 160) \text{ mwe}$   
 $\langle R_\mu \rangle = (800 \pm 10) \text{ d}^{-1}$



Average muon rate as a function of time, computed using a 30-day width Hamming moving average window. The colored surface delimits the 95% confidence interval. Gray bar indicate periods where the acquisition was interrupted for work in the Mont Terri URL.

# Results - Muon monitoring

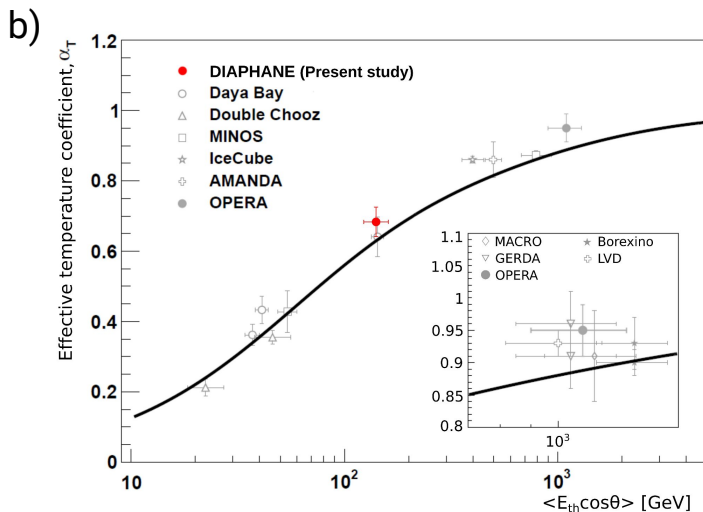
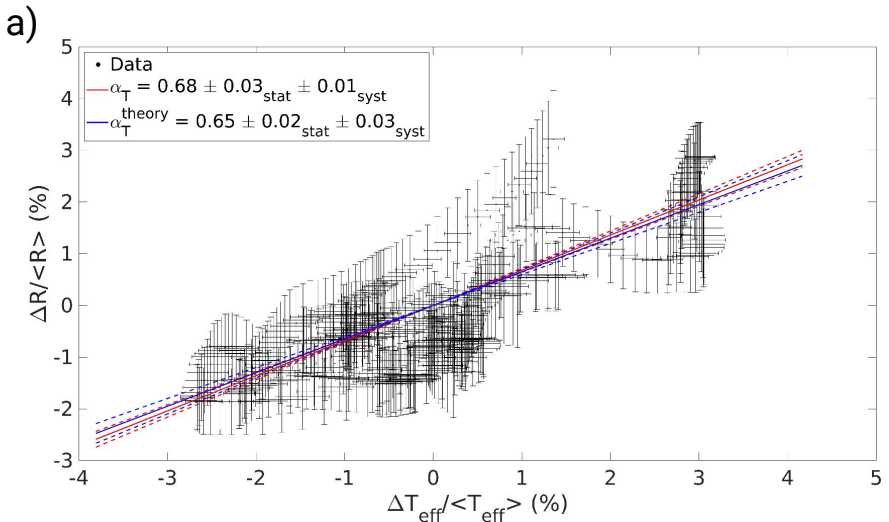
- We have found the variation in thermal state of the atmosphere to be a significant cause of the observed muon rate variations.



Daily percent deviations from the mean of the average muon rate, the daily effective temperature, and the average effective temperature computed using a 30 days width Hamming window. The colored surfaces delimit the 95% confidence interval associated to each curve

# Results - Muon monitoring

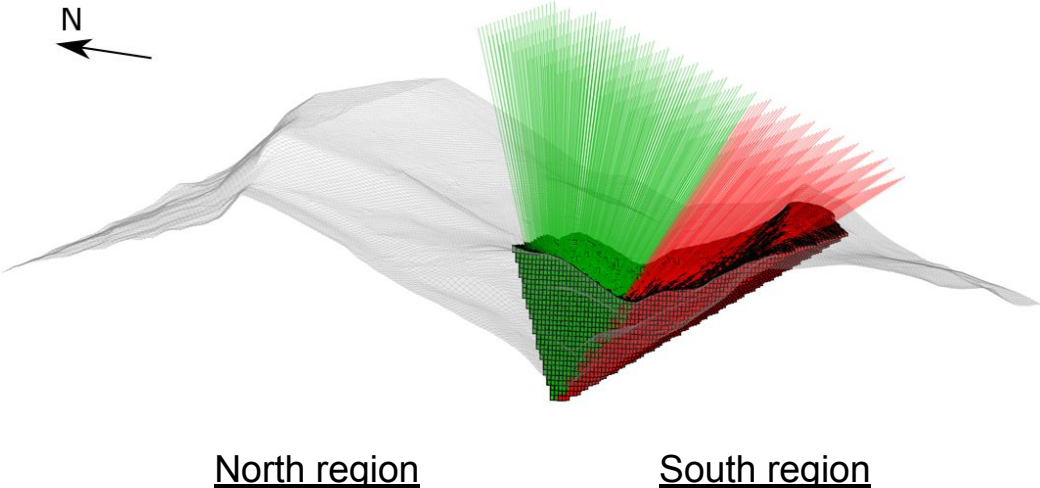
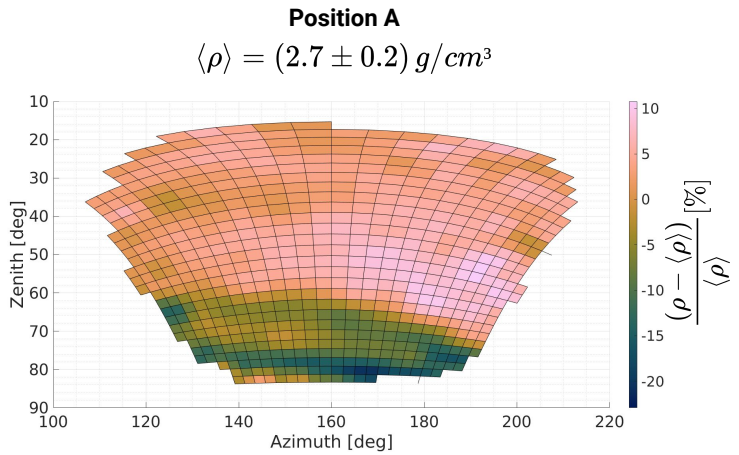
- We determined the effective temperature coefficient to be  $\alpha_T = 0.68 \pm 0.03_{\text{stat}} \pm 0.01_{\text{syst}}$ .



a) Average muon rate relative variation versus average effective temperature relative variation. b) Experimental values of the effective temperature coefficient. The continuous black line represents a theoretical model. Figure adapted from Agafonova et al. (2018)

# Results - Muon monitoring

- Based on the muon radiography, by merging adjacent axis of observation, we study the North Region and the South Region separately.



North region

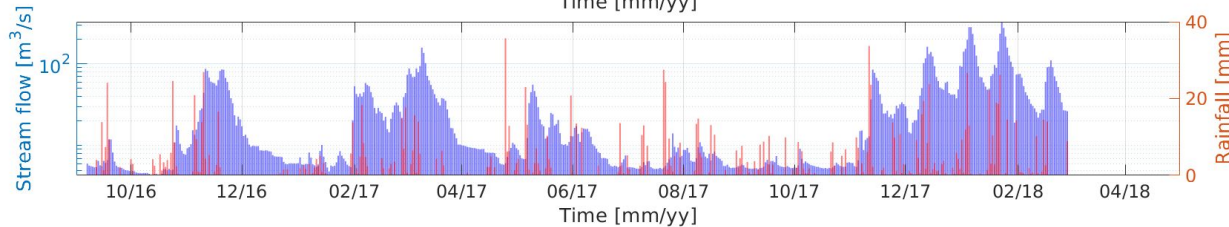
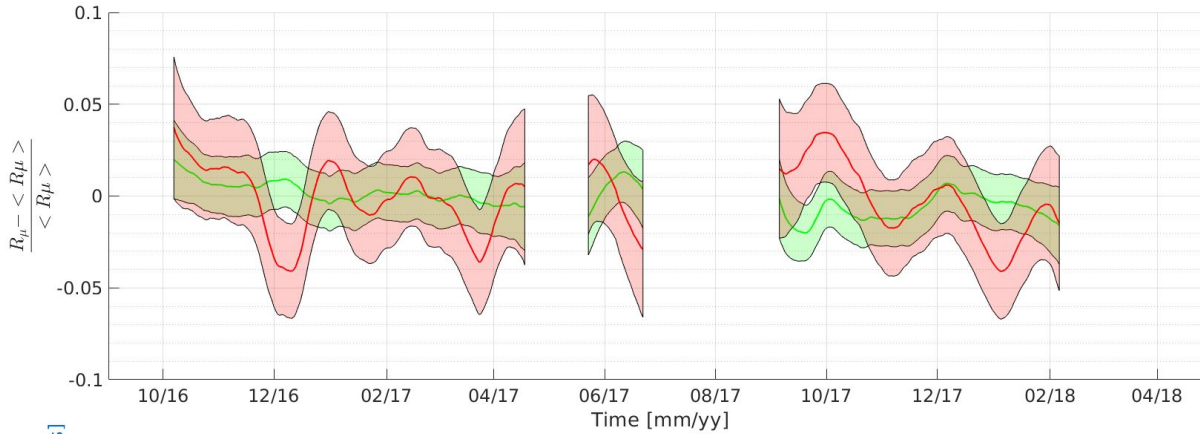
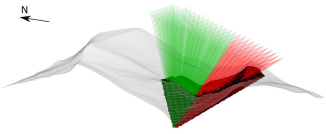
South region

Volume:  $\sim 4.0 \times 10^6 \text{ m}^3$   
 $\langle \rho \rangle = (605 \pm 45) \text{ mwe}$   
 $\langle R_\mu \rangle = (605 \pm 7) \text{ d}^{-1}$

Volume:  $\sim 7.7 \times 10^6 \text{ m}^3$   
 $\langle \rho \rangle = (795 \pm 200) \text{ mwe}$   
 $\langle R_\mu \rangle = (195 \pm 5) \text{ d}^{-1}$

# Results - Muon monitoring

- Filtered muon rate variations in the North and the South region.



# Results - Muon monitoring

**First order hydrological modelling to define mass balance at hillslope scale.**

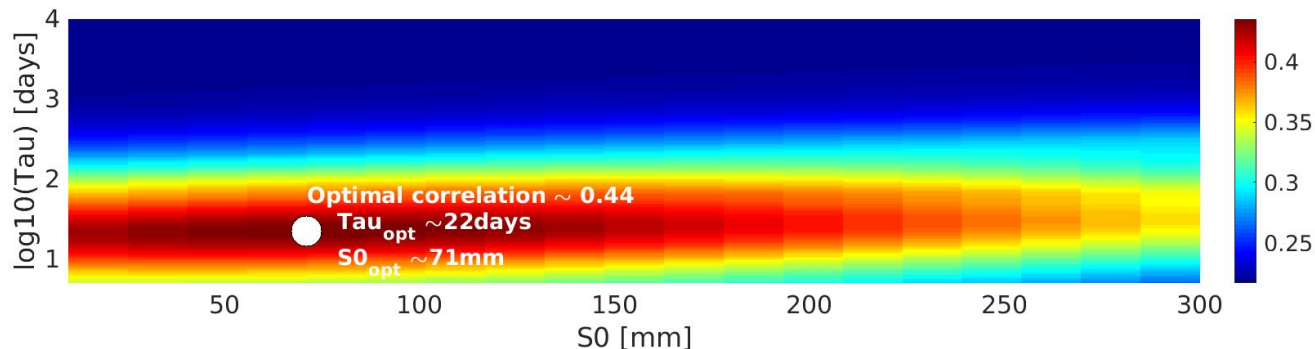
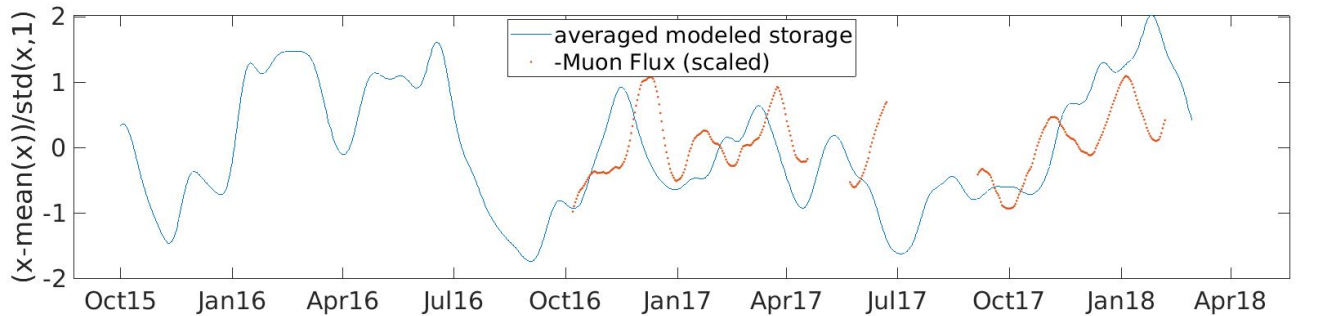
*Collaboration with L. Longuevergne, CNRS-Géosciences Rennes, France.*

- We resolve at daily time scale:

$$\left\{ \begin{array}{l} \frac{dS}{dt} = P - E - Q \\ Q = \frac{S}{\tau} \end{array} \right. \quad \begin{array}{l} S : \text{storage} \\ Q : \text{discharge} \\ P : \text{precipitation} \\ E : \text{evapotranspiration} \\ \tau : \text{linear outflow parameter} \end{array}$$

- Recharge is input data, and the initial storage  $S_0$  and  $\tau$  are input parameters.
- We fit the optimal  $S_0$  and  $\tau$  that result in the highest cross-correlation between the 30-day averaged modeled storage  $S$  and  $-\left(\frac{\Delta R}{\langle R \rangle}\right)_{filtered}$  in the South Region.

# Results - Muon monitoring



# Outline

- Introduction
- Methodology
- Results
- Conclusions

- Based on the muon radiography, we identify regions with distinct average densities. The high-density region contains a local aquifer with higher inflow rates, and the low-density region contains both the local aquifer and the regional one, with lower inflow rates.
- The continuous muon data suggest that the high-density region experiences smaller variations of water content. This may be due to the higher inflow rates. On the other hand, the large variability observed in the region to the south of the valley may be due to lower inflow rates causing underground water to accumulate and discharge over longer time scales.

Thank you  
for your attention !

[mtramontini@fcaglp.unlp.edu.ar](mailto:mtramontini@fcaglp.unlp.edu.ar)